# Combined Effects on Selectivity in Fe-Catalyzed Methylene Oxidation

Mark S. Chen and M. Christina White

*Science* **327**, 566 (2010);
DOI: 10.1126/science.1183602



*Science* (print ISSN 0036-8075; online ISSN 1095-9203) is published weekly, except the last week in December, by the American Association for the Advancement of Science, 1200 New York Avenue NW, Washington, DC 20005. 

region around the $Si_4$ ring with a bifurcation threshold (0.755) similar to that reported for homoaromatic carbon rings (*32*). This feature is also present in the ELF isosurface, including just HOMO to HOMO−3. When the HOMO−1 is excluded, the ELF surface now starts to resemble the topology of the torus link computed using the π-MOs of benzene (*33*).

In order to quantify the aromaticity of **3a,b**, we calculated the nucleus-independent chemical shift, NICS(0), at the center of the $Si_4$ ring of **3b** (−23.8 ppm), which indicates substantial aromaticity (benzene ~ −10 ppm) but may also include shielding effects from the σ-framework (*34*). To estimate these latter effects, we computed the NICS(0) value for **4,** the hypothetical saturated hydrogenation product of **3b**. This in silico reduction has the effect of sequestering the two Si lone pair electrons and hence suppressing the dismutational resonance. The result (−6.4 ppm) suggests that the strongly diatropic NICS(0) value of **3b** is truly due to aromaticity. Further confirmation is obtained from the NICS(0) value of −3.3 ppm for the $^3A_u$ triplet (and presumed nonaromatic) state of **3b** (resonance **C**) (Scheme 2).

In order to place **3b** in terms of relative energy, we calculated two of its isomers with Dip substituents: the experimentally known hexasilaprismane (*18*) and the hypothetical hexasilabenzene. Both turned out to be lower in free energy $\Delta G_{298}$ [B3LYP/6-31G(d); **3b**, 0.0; prismane, −11.7; benzene, −4.3 kcal $mol^{-1}$] with the hexasilabenzene surprisingly situated midway, which raises the intriguing possibility of a future synthesis of a stable hexasilabenzene.

The general formalism leading to the type of aromaticity exemplified by **3a-c** is a twofold formal 1,2-shift of substituents in the classical Hückel aromatic compounds: a double intramolecular dismutation. The formal oxidation states of the silicon atoms in **3a-c** are +2 ($SiR_2$), +1 (SiR), and 0 (Si) as opposed to the uniform oxidation state of +1 in hexasilabenzenes. We propose the term dismutational aromaticity for a phenomenon that in principle should be applicable to any classical Hückel aromatic compound with at least six ring atoms.

### References and Notes


1. M. Faraday, *Philos. Trans. R. Soc. Lond. B Biol. Sci.* **115**, 440 (1825).
2. W. von E. Doering, F. L. Detert, *J. Am. Chem. Soc.* **73**, 876 (1951).
3. A. T. Balaban, P. R. Schleyer, H. S. Rzepa, *Chem. Rev.* **105**, 3436 (2005).
4. T. C. Dinadayalane, U. D. Priyakumar, G. N. Sastry, *J. Phys. Chem. A* **108**, 11433 (2004).
5. F. A. Cotton, G. Wilkinson, *Advanced Inorganic Chemistry* (Wiley, New York, ed. 4, 1980).
6. R. West, M. J. Fink, J. Michl, *Science* **214**, 1343 (1981).
7. M. Kira, T. Iwamoto, *Adv. Organomet. Chem.* **54**, 73 (2006).
8. A. Sekiguchi, R. Kinjo, M. Ichinohe, *Science* **305**, 1755 (2004).
9. T. Sasamori *et al.*, *J. Am. Chem. Soc.* **130**, 13856 (2008).
10. V. Y. Lee, A. Sekiguchi, *Angew. Chem. Int. Ed.* **46**, 6596 (2007).
11. K. Wakita, N. Tokitoh, R. Okazaki, S. Nagase, *Angew. Chem. Int. Ed.* **39**, 634 (2000).
12. R. Kinjo *et al.*, *J. Am. Chem. Soc.* **129**, 7766 (2007).
13. M. Ichinohe, M. Igarashi, K. Sanuki, A. Sekiguchi, *J. Am. Chem. Soc.* **127**, 9978 (2005).
14. V. Y. Lee, K. Takanashi, T. Matsuno, M. Ichinohe, A. Sekiguchi, *J. Am. Chem. Soc.* **126**, 4758 (2004).
15. M. J. S. Dewar, D. H. Lo, C. H. Ramsden, *J. Am. Chem. Soc.* **97**, 1311 (1975).
16. S. Nagase, H. Teramae, T. Kudo, *J. Chem. Phys.* **86**, 4513 (1987).
17. K. K. Baldridge, O. Uzan, J. M. L. Martin, *Organometallics* **19**, 1477 (2000).
18. A. Sekiguchi, T. Yatabe, C. Kabuto, H. Sakurai, *J. Am. Chem. Soc.* **115**, 5853 (1993).
19. K. Abersfelder, D. Scheschkewitz, *J. Am. Chem. Soc.* **130**, 4114 (2008).
20. D. Scheschkewitz, *Angew. Chem. Int. Ed.* **44**, 2954 (2005).
21. D. Scheschkewitz, *Angew. Chem. Int. Ed.* **43**, 2965 (2004).
22. Materials and methods are available as supporting material on *Science* Online and contain details of experimental procedures, analytical data, and x-ray structure determinations. Details of the computational procedures are available via the interactive table and the digital repository links therein. Regarding general information on the digital repository, see (*35*).
23. L. Shimoni-Livny, J. P. Glusker, C. W. Bock, *Inorg. Chem.* **37**, 1853 (1998).
24. A. Schnepf, *Chem. Soc. Rev.* **36**, 745 (2007).
25. G. Fischer *et al.*, *Angew. Chem. Int. Ed.* **44**, 7884 (2005).
26. Q. Zhang *et al.*, *J. Am. Chem. Soc.* **131**, 9789 (2009).
27. E. Niecke, A. Fuchs, F. Baumeister, M. Nieger, W. W. Schoeller, *Angew. Chem. Int. Ed. Engl.* **34**, 555 (1995).
28. M. Seierstad, C. R. Kinsinger, C. J. Cramer, *Angew. Chem. Int. Ed.* **41**, 3894 (2002).
29. T. Schepers, J. Michl, *J. Phys. Org. Chem.* **15**, 490 (2002).
30. R. F. W. Bader, *Atoms in Molecules: A Quantum Theory* (Oxford Univ. Press, Oxford, 1990).
31. A. Savin *et al.*, *Angew. Chem. Int. Ed. Engl.* **31**, 187 (1992).
32. C. S. M. Allan, H. S. Rzepa, *J. Chem. Theory Comput.* **4**, 1841 (2008).
33. C. S. Wannere *et al.*, *J. Phys. Chem. A* **113**, 11619 (2009).
34. Z. Chen, C. S. Wannere, C. Corminboeuf, R. Puchta, P. R. Schleyer, *Chem. Rev.* **105**, 3842 (2005).
35. J. Downing *et al.*, *J. Chem. Inf. Model.* **48**, 1571 (2008).


36. We thank the Deutsche Forschungsgemeinschaft (DFG SCHE 906/3-2) and the Karl-Winnacker-Fund of the Aventis Foundation for financial support. Crystallographic details were deposited with the Cambridge Crystallographic Data Centre as CCDC-745660 (**2**) and 745661 (**3a**).


### Supporting Online Material

www.sciencemag.org/cgi/content/full/327/5965/564/DC1
Materials and Methods
Figs. S1 to S6
Reference
Interactive Table

10 September 2009; accepted 24 November 2009
10.1126/science.1181771

# Combined Effects on Selectivity in Fe-Catalyzed Methylene Oxidation

**Mark S. Chen and M. Christina White***

**Methylene C–H bonds are among the most difficult chemical bonds to selectively functionalize because of their abundance in organic structures and inertness to most chemical reagents. Their selective oxidations in biosynthetic pathways underscore the power of such reactions for streamlining the synthesis of molecules with complex oxygenation patterns. We report that an iron catalyst can achieve methylene C–H bond oxidations in diverse natural-product settings with predictable and high chemo-, site-, and even diastereoselectivities. Electronic, steric, and stereoelectronic factors, which individually promote selectivity with this catalyst, are demonstrated to be powerful control elements when operating in combination in complex molecules. This small-molecule catalyst displays site selectivities complementary to those attained through enzymatic catalysis.**

Methylene (secondary) C–H bonds are ubiquitous in organic structures and are often viewed by organic chemists as the inert scaffold upon which the traditional chemistry of "reactive" functional groups is performed. In contrast, the enzymatic oxidation of methylenes (i.e., C–H to C–O) is a fundamental transformation in biological systems and is critical for drug metabolism and the biosynthesis of secondary metabolites (*1*, *2*). Selectivity in enzymatic catalysis is dictated by the local chemical environment of the enzyme active site, a feature that inherently limits substrate scope. Despite important advances in the discovery of catalysts for C–H oxidation, the ability to directly functionalize isolated, unactivated secondary C–H bonds with useful levels of selectivity in complex molecule settings under preparatively useful conditions (i.e., limiting amounts of substrate) has been restricted to the realm of enzymatic catalysis. A small-molecule catalyst capable of performing methylene oxidations with broad scope, predictable selectivities, and in preparatively useful yields would have a transformative effect on streamlining the practice of organic synthesis.

The paucity of methods for the oxidation of isolated, unactivated, and nonequivalent secondary C–H bonds underscores that they are, arguably, the most challenging chemical bonds to selectively functionalize. Reactivity for oxidizing such bonds had been observed with several catalysts, but generally in substrates where selectivity issues are circumvented (e.g., cyclohexane → cyclohexanone) (*3*–*11*) or else where reactive sites are either electronically activated (i.e., adjacent

Department of Chemistry, Roger Adams Laboratory, University of Illinois, Urbana, IL 61801, USA.

*To whom correspondence should be addressed. E-mail: white@scs.uiuc.edu

to π-systems or heteroatoms) (*12*–*15*) or oriented favorably toward a directing group (*16*–*19*). The electron-rich nature of tertiary C–H bonds and their relative scarcity makes them more facile targets for selective oxidation (*3*–*5*, *19*, *20*). Bio-inspired catalysts with elaborate binding pockets have been viewed as the most promising candidates to effect site selectivity in unactivated, non-directed methylene oxidations (*21*).

We recently reported a bulky, electrophilic catalyst [Fe(*S,S*-PDP) **1**] (Fig. 1C) (*3*, *4*) that uses $H_2O_2$ with acetic acid as an additive (*22*) to stereospecifically oxidize isolated, unactivated tertiary C–H bonds across a broad range of substrates. Surprisingly, predictably high levels of site selectivity were shown to be possible with **1** based on subtle steric and electronic differences among multiple tertiary C–H bonds. Encouraged by these results, we hypothesized that such a catalyst that is highly responsive to a combination of electronic and steric effects would be well suited for selective secondary C–H bond oxidation. Chemoselectivity advantages for secondary C–H bond oxidation may arise from increased steric accessibility compared to tertiary C–H bonds and greater electron-rich character compared to primary C–H bonds (Fig. 1A). Because secondary C–H bonds have intermediate electronic properties, they may be particularly amenable to tuning by both electronic activation and deactivation. Moreover, since secondary C–H bonds are prevalent in ring systems, a variety of stereoelectronic effects (i.e., the influence of orientation of electron orbitals in space on chemical reactivity) may be readily exploited to achieve high site selectivity in their functionalization.

Here, we report that the same bulky, electrophilic Fe(*S,S*-PDP) **1** catalyst is capable of site-selective oxidation of isolated, unactivated secondary C–H bonds to afford mono-oxygenated products in preparatively useful yields—without the use of directing or activating groups. The site selectivities can be predicted in complex molecular settings on the basis of steric, electronic, and stereoelectronic rules derived from simple compounds. Whereas individually these effects in some cases afford modest selectivity, when manifest in combination in natural-product settings they result in useful levels of chemo-, site-, and even diastereoselective methylene oxidations (Fig. 1B). Moreover, because site selectivity in the case of small-molecule catalyst **1** is driven by its sensitivity to the local chemical environment of the substrate, we can achieve site selectivities complementary to those obtained in biotransformations.

The highly electrophilic oxidant generated with (*S,S*)-**1** and $H_2O_2$ allows for substantial electronic control over secondary C–H oxidation site selectivities (Fig. 2). *n*-Hexane, a hydrocarbon with no electronic biasing elements, is oxidized with no site selectivity (primary C–H bond oxidation has not been observed with **1**), forming ketones **2** and **3** in equal amounts (Fig. 2, entry 1) (*23*). The oxidation of methylene C–H bonds furnishes ketone products through alcohol intermediates via two stepwise, rapid oxidations (alcohols have been detected under conditions of limiting oxidant). A single electron-withdrawing group (EWG), such as a terminal ester, deactivates proximal sites via inductive effects, thereby introducing differential electronic environments that bias the site of oxidation. Specifically, high selectivity for ketone formation is observed at the most electron-rich methylene site (~50% yield), corresponding to that farthest from the EWG (entries 2 to 5). Consistent with our expectations (see above), the electronic biasing effect on methylene oxidations with (*S,S*)-**1** appears to be very strong; electronic deactivation by the ester

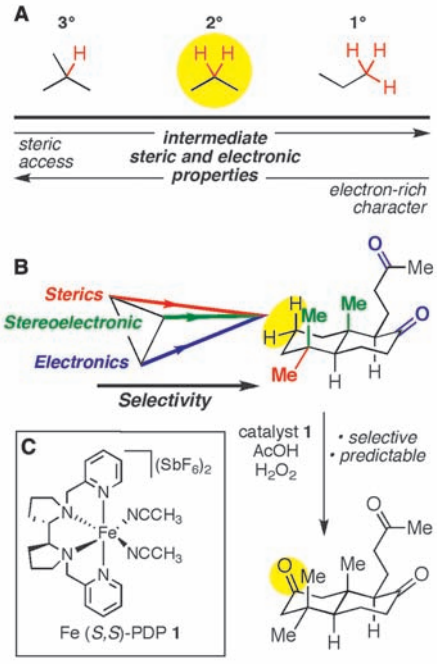


**Fig. 1.** (**A**) Chemical properties of aliphatic C-H bonds. (**B**) Synergistic effects on site selectivity. Steric, stereoelectronic (influence of orientation of electron orbitals in space on reactivity), and electronic influences on reactivity with catalyst **1** have an additive effect in complex molecule settings, which can lead to highly predictable and selective outcomes. (**C**) Electrophilic, bulky catalyst Fe(*S,S*)-PDP (**1**) for predictably selective aliphatic C–H oxidation.

**Fig. 2.** Electronic influences (inductive effects) on site selectivity in the oxidation of secondary C–H bonds of acyclic and cyclic substrates. An iterative addition protocol was used in which catalyst **1**, $H_2O_2$ oxidant, and AcOH additive were added in three portions over a 30-min period to decrease the rate of bi- or multimolecular catalyst decomposition relative to substrate oxidation (*3*, *4*, *23*). Methylene C–H oxidation with **1** occurs preferentially at the methylene site most remote from EWGs; rsm, % recovered unoxidized starting material. The average mass balance for entries 2 to 13 is 94%.

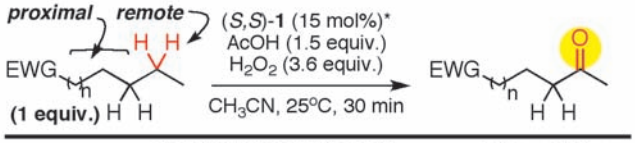


| Entry | Major Oxidation Product Isolated % Yield† (%rsm) | Sites of Minor Oxidation % Yield |
|---|---|---|
| 1 | **2** + **3** 56%‡ ( - ) [**2**:**3**] = 1.1:1 | --- |
| 2 | **4**, 50% (22%) | C4, 22% |
| 3 | **5**, 51% (16%) | C5, 18%<br>C4, 14% |
| 4 | **6**, 54% (23%) | C4, 15%<br>C2, 1%‡ |
| 5 | **7**, 43%§ (22%) | C4, 14%<br>C3, 9% |
| 6 | **8**, R = O 0 % (98%) | --- |
| 7 | **9**, R = OPiv 30% (41%) | C2, 14% |
| 8 | **10**, R = $CO_2$Me 52% (37%) | C2, 2% |
| 9 | **11**, R = $CH_2$OPiv 60%¶ (28%) | C2, 9% |
| 10 | **12**, R = O 38% (33%) | C3, 25% |
| 11 | **13**, R = OPiv 50% (22%) | C3, 24% |
| 12 | **14**, R = $CO_2$Me 45% (20%) | C3, 28% |
| 13 | **15**, R = $CH_2$OPiv 43% (14%) | C3, 37% |

* Iterative addition protocol. † Unless otherwise noted, all compounds were isolated as single oxidized products. ‡ GC yield. § Isolated in 52% yield as an inseparable 5:1 mixture of [C5:C3] oxidation products. ¶ Isolated in 69% yield as an inseparable 7:1 mixture of [C3:C2] ketones.

moiety in methylheptanoate **5** results in high selectivity for oxidation at the remote C-6 position relative to four other proximal secondary sites (entry 3, 51% yield). When tertiary sites are positioned α or β to EWGs, the above trend still holds, highlighting the utility of this tactic for effecting the chemoselective oxidation of secondary C–H bonds in preference to tertiary C–H bonds (entries 4 and 5).

Electronic deactivation of proximal methylene sites also leads to predictably selective outcomes for oxidations within five- and seven-membered ring systems. In all cases examined, the major product is a result of ketonization at the methylene site most remote from the EWG (Fig. 2, entries 6 to 13). Consistent with selectivity trends found with acyclic substrates, cyclopentanone shows no conversion due to strong electronic deactivation of secondary sites α or β to the carbonyl (entry 6). Increased product formation as high as 60% (**11**, entry 9) is observed as the EWG is rendered less inductively withdrawing and/or more remote from the ring (entries 7 to 9). Similar reactivity trends are observed with the oxidation of seven-membered rings; however, the benefits of an EWG on site selectivities are less pronounced (entries 10 to 13). For example, as the EWG is rendered less inductively withdrawing, the increased reactivity is offset by the erosion of site selectivity due to increased oxidation at the more proximal C3 position (entries 12 and 13). This trend reveals that a careful balance between substrate reactivity and selectivity must be struck when relying on electronic deactivation alone to achieve site selectivity with these simple substrates.

Examination of a series of six-membered cyclic substrates with EWGs demonstrated no preference for the more electronically favored C4 methylene site over the more proximal C3 site (Fig. 3A, entries 1 and 2). However, an increase in [C3:C4] site selectivity was observed with a sterically bulkier ring substituent that was no longer electronically deactivating (i.e., *tert*-butyl, entry 3). These trends suggest that stereoelectronic parameters based on conformational effects are strong contributing factors to the observed product distribution in six-membered ring oxidations with **1** (entries 1 to 3). In these cases, torsional strain between the bulky equatorial group and vicinal methylenes, generated by unfavorable 1,3-diaxial interactions at C1 and C3, is alleviated upon C3 C–H oxidation (*24*). In addition, such sterically bulky substituents also contribute to selectivity by inhibiting oxidation at adjacent sites. Methylene sites adjacent to bulky *t*-butyl or *gem*-dimethyl groups are disfavored in oxidations with (*S,S*)-**1**; α positions are consistently oxidized in the lowest statistical yields (2% C2-ketone, entry 3; Fig. 3B, entry 4).

The bulky nature of the (*S,S*)-**1** catalyst even allows for subtle steric influences to have notable effects on the chemoselectivity of secondary versus tertiary C–H bond oxidations (Fig. 3B, entries 5 and 6). *cis*-Isomer **29**, containing equatorial tertiary sites, undergoes preferential tertiary hydroxylation to provide alcohol **30** in 55% yield (tertiary:secondary = 4:1, entry 5). In contrast, oxidation of *trans*-isomer **33**, containing only axial tertiary sites, affords predominantly secondary C–H bond oxidation products **35** and **36** in a combined 50% yield (tertiary:secondary = 1:2, entry 6). Although a preference for equatorial versus axial tertiary C–H bond oxidation has been noted for dioxirane oxidants (*5*), a reversal in chemoselectivity to favor secondary C–H bond oxidation has not been previously reported. This is most likely because the strong electronic preference for tertiary hydroxylation with an electrophilic oxidant can be overridden only with a very bulky oxidant

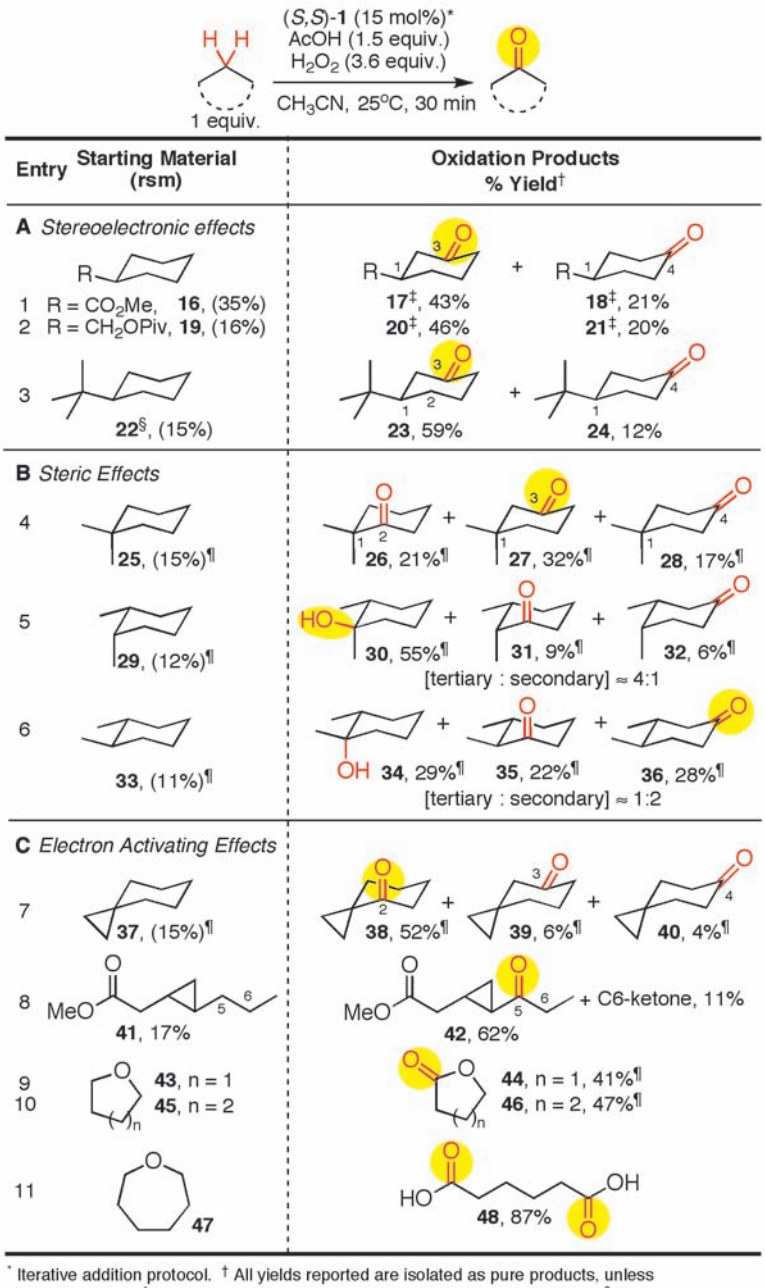


* Iterative addition protocol. † All yields reported are isolated as pure products, unless otherwise noted. ‡ Isolated as an inseparable mixture of C3- and C4-ketones. § C2-ketone was observed in 2% GC yield. ¶ Yield determined by GC analysis.

**Fig. 3.** Stereoelectronic, steric, and electronic influences (hyperconjugative activation) on chemoselectivity and site selectivity in the oxidation of secondary C–H bonds in six-membered rings. (**A**) Alleviation of torsional ring strain in six-membered rings favors formation of C3- over C4-ketone products. Average mass balance for entries 1 to 3 is 89%. (**B**) Steric factors can lead to both site selectivity and chemoselectivity for secondary C–H bond oxidation in preference to tertiary C–H bonds with bulky catalyst **1**. The average mass balance for entries 4 to 6 is 86%. (**C**) Electron activation (via hyperconjugation) of aliphatic secondary C–H bonds for site-selective methylene oxidation; rsm, % recovered unoxidized starting material.

like that formed with catalyst (*S,S*)-**1**/$H_2O_2$. We hypothesized that the collective influence of these individual steric effects on site selectivity can have a combined effect on the selective oxidation of substrates with increased conformational rigidity (see below).

Although not required, electronic activating groups (EAGs) can be used to achieve site selectivities with catalyst **1** that are orthogonal to those based on inductive or steric effects (Fig. 3C). Groups capable of hyperconjugative activation, i.e., donation of electron density from a filled orbital to the antibonding orbital of a C–H bond, may be used to activate adjacent C–H bonds toward oxidation. The strained cyclopropane ring, having appreciable p-character in the C–C bonding orbitals, can activate the cyclopropylcarbinyl methylenes through hyperconjugation (*25*). For example, cyclopropanes can direct secondary C–H bond oxidations at sites that are sterically or inductively deactivated. Although quaternary alkyl substitution diverts oxidation away from α-hydrogens on a cyclohexane ring (Fig. 3B, entry 4), selective oxidation at these sites occurs when a cyclopropyl group is installed (Fig. 3C, entry 7). The site selectivity in the oxidation of methylheptanoate can also be altered to favor the C5 position (disfavored based on inductive effects: Fig. 2, entry 3, C5:C6 = 1:3) via the incorporation of a cyclopropyl moiety (Fig. 3C, entry 8, C5:C6 = 6:1). Following the previously established electronic trends, the more electron-rich of the two methylene sites flanking the cyclopropyl ring is still selectively oxidized. No oxidation of tertiary C–H bonds on the cyclopropyl ring was observed. Another powerful form of hyperconjugative activation is the interaction of lone-pair electrons of an ethereal oxygen with adjacent C–H bonds (*26*, *27*). This electronic activating effect enables the selective oxidation of five- and six-membered cyclic ethers into lactone products (entries 9 and 10). Lower product yields and poor mass balance in these cases can be attributed to overoxidation of the open-chain hydroxyaldehyde form of the intermediate lactol. Consistent with this explanation, when a seven-membered cyclic ether is oxidized, lactone is not observed but adipic acid (**48**) is

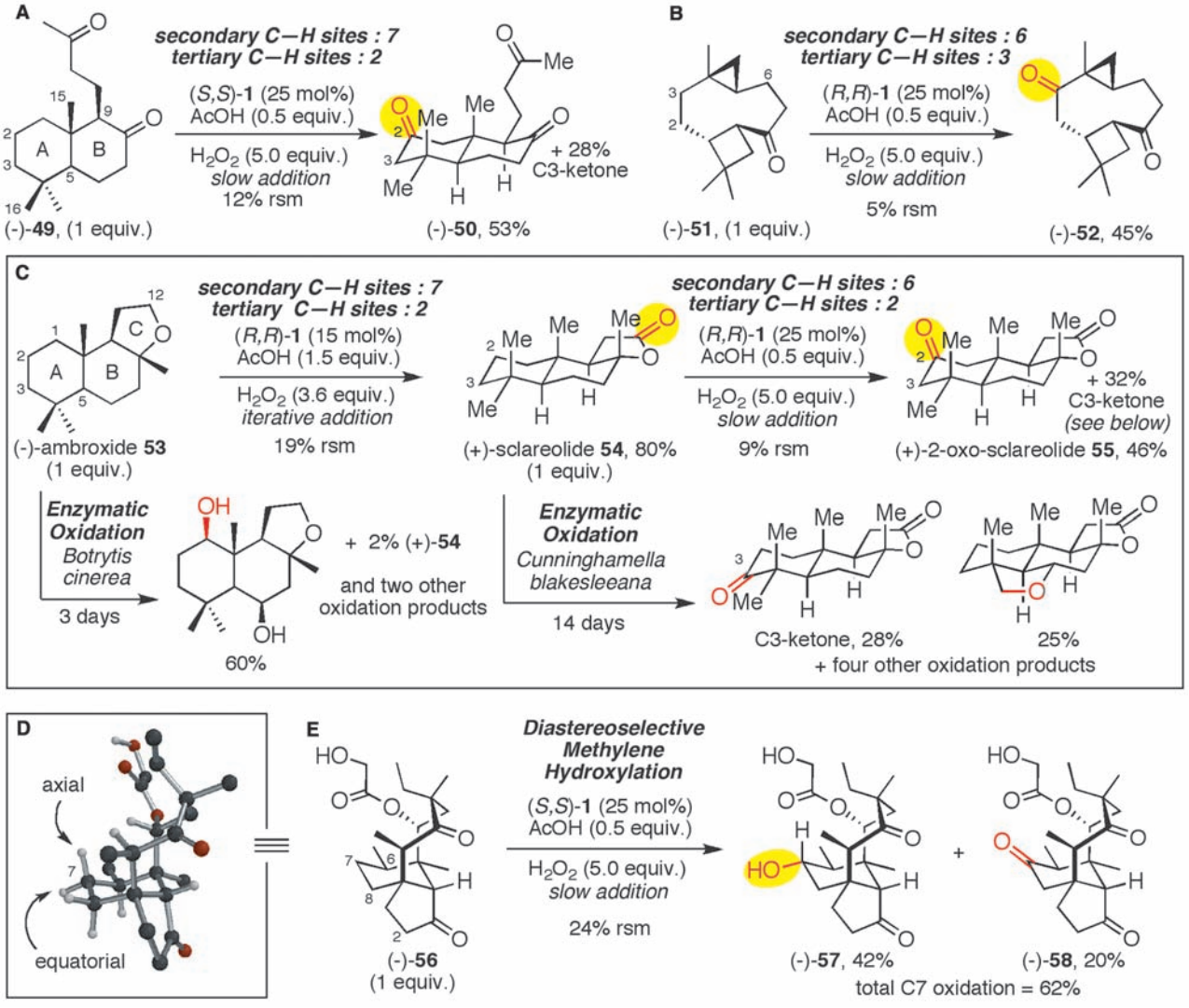


**Fig. 4.** Additive effects of steric, electronic, and stereoelectronic factors on the selectivity of secondary C-H bond oxidations of terpenoids. A slow addition protocol was used in which catalyst **1** and $H_2O_2$ oxidant were added via syringe pump over a 1-hour period to decrease the rate of bi- or multimolecular catalyst decomposition relative to substrate oxidation (*4*, *23*). (**A**) Electronic and steric deactivation, as well as stereoelectronic activation via alleviation of 1,3-diaxial six-membered ring interactions, lead to predictable and highly selective oxidations by **1** on manool-derived dione (–)-**49**. (**B**) Cyclopropane-induced methylene activation (via hyperconjugative electron activation), as well as electronic deactivation, leads to selective oxidation of (–)-**51**. (**C**) Transformation of (–)-ambroxide (**53**) into (+)-**55** via sequential, intermolecular secondary C–H oxidation. Microbial biotransformations of (–)-**53** and (+)-**54** demonstrate site selectivities orthogonal to those of Fe(*R,R*-PDP) **1**. For a complete list of all the oxidation products formed in the microbial oxidations, see figs. S1 and S2 (*23*). (**D**) Energy-minimized structure of (–)-dihydropleuromutilone (**56**). (**E**) Diastereoselective methylene hydroxylation of (–)-**56**; rsm, % recovered unoxidized starting material.

isolated in 87% yield (entry 11). In more conformationally rigid substrates, overoxidation is not observed (see below). Benzylic sites are also activated toward selective oxidation, although this effect is limited by the requirement for EWG substitution on the aromatic ring to prevent its oxidation (compound *S1*) (*23*).

Having established a framework of selectivity rules for catalyst **1** with relatively simple molecules, we sought to apply the system to complex natural products. In this respect, we sought to mimic the action of selective oxidative enzymes like the cytochrome P-450s. Terpenoids, the largest and most diverse class of natural products, are biosynthesized through pathways that introduce oxygen functionality independent of C–C bond–forming events. Topologically diverse hydrocarbon skeletons are forged through a sequence of carbonyl condensations, reductions that remove postcondensation oxygen functionality, and cyclizations (*28*). Oxidation patterns are subsequently installed via late-stage oxidative tailoring enzyme modifications (*1*). We hypothesized that the individual electronic, steric, and stereoelectronic effects on selectivity in oxidations of simple compounds with catalyst **1** (see above) would be heightened when combined in complex molecule settings.

We first examined the oxidation of dione (−)-**49**, a molecule derived from the diterpenoid (+)-manool, that comprises a substituted *trans*-decalin core and contains a total of 28 C–H bonds, 14 of which are secondary and two tertiary (Fig. 4A). According to our selectivity rules, we hypothesized that the two tertiary sites should be electronically and sterically deactivated toward oxidation: C9 is α to a ketone, and C5 is both in an axial orientation and adjacent to a *gem*-dimethyl group. With regards to methylene oxidation, we recognized that the two ketones electronically deactivate the side chain and the entire B ring, leaving the secondary C–H bonds of the A ring as the most likely sites for oxidation. The most distal site from the sterically bulky quaternary centers on the A ring is C2; moreover, repulsive 1,3-diaxial interactions with two methyl substituents (C15 and C16) may be relieved by C2 C–H bond oxidation. Despite nine possible sites of oxidation, we observed oxidation at only the C2 and C3 sites. Consistent with our analysis, C2 is the major site of oxidation affording (−)-**50** in 53% isolated yield (12% recovered starting material, rsm). This example highlights the capacity for distinct selectivity factors to become mutually reinforcing in a complex molecule setting, thereby producing predictable and highly selective oxidation of secondary C–H bonds.

Site selectivity through hyperconjugative activation is demonstrated with the Fe(PDP)-catalyzed oxidation of the terpenoid derivative (−)-**51**, a compound with a sensitive carbogenic framework composed of a cyclopropane- and cyclobutane-annulated nine-membered ring (Fig. 4B). We hypothesized that the cyclopropane moiety would effectively override steric effects and activate the two adjacent methylene groups, with C3 being favored for oxidation relative to C6 because of its remoteness from the ketone moiety. Upon exposure of (−)-**51** to catalyst **1**, a number of minor, unidentified oxidation products were observed; however, oxidation at C3 occurred preferentially to furnish ketone (−)-**52** as the major product in a preparatively useful 45% yield (5% rsm). This oxidation proceeds in higher yield and selectivity with (*R,R*)-**1** than (*S,S*)-**1**, which we rationalize as a better matching of catalyst geometry with substrate topology.

Selective, sequential oxidations (*27*) may be achieved with an electrophilic oxidant by engaging an electron-activating group, in an otherwise electronically unbiased hydrocarbon skeleton, to direct the initial site of oxidation. Upon oxidation, the newly installed ketone, acting as an EWG, will inductively bias the molecule during further oxidation. The two-step oxidative transformation of (−)-ambroxide (**53**) into (+)-2-oxo-sclareolide (**55**) demonstrates the power of this strategy to effect highly selective sequential oxidations with (*R,R*)-**1** (Fig. 4C). The first methylene oxidation exploits the activated C–H bonds on the five-membered cyclic ether (C ring) to achieve high site selectivity at one site among nine other possible sites of oxidation. Oxidation of the α-ethereal C–H bonds furnishes (+)-(3*R*)-sclareolide (**54**) in 80% yield, even amid numerous other electronically and sterically accessible secondary and tertiary sites of oxidation. The newly installed lactone of (+)-**54** now serves as an EWG to inductively deactivate the B and C rings, making the secondary C–H bonds on the A ring most favorable toward further oxidation. As noted above with an analogous *trans*-decalin structure [(−)-**49**], C2 and C3 are the only notable sites of oxidation with catalyst **1**/$H_2O_2$. Among these two sites, C2 is favored on the basis of destabilizing diaxial interactions and results in (+)-2-oxo-sclareolide (**55**) being the major oxidation product in 46% isolated yield (9% rsm). Oxidation of (−)-**53** with catalyst **1** afforded very little yield of (+)-**55**, even at higher catalyst and oxidant loadings. This observation suggests that rapid catalyst decomposition may play a role in preventing overoxidations with this mild oxidant (*4*). Through an interplay of electronic activation and deactivation, opposite hemispheres of a complex molecule can be selectively oxidized through intermolecular oxidation steps with a single catalyst. Oxidations of (−)-**53** and (+)-**54** with microbial enzymes, which are reported to furnish some of the oxidation products we observe with catalyst **1**, require substantially longer reaction times (3 to 14 days), provide (+)-**54** from (−)-**53** in only minimal yield (<5%), and demonstrate no observable formation of (+)-**55** from (+)-**54** (Fig. 4C) (*29*, *30*). These examples illustrate that site-selective oxidations can be predictably achieved with catalyst **1** that are often complementary to those accessible via enzymatic oxidations.

Pleuromutilin and its derivatives have attracted extensive attention from both the pharmaceutical and academic communities because of their potent activities against drug-resistant Gram-positive bacteria and their unusual tricyclic diterpenoid structure. Despite potent antibacterial activities, their hydrophobic nature limits their solubility and promotes rapid degradation by cytochrome P-450 at the C2 and C8 positions, resulting in inactive metabolites (*31*). On the basis of our findings with (−)-**53** and (+)-**54**, we anticipated that catalyst (*S,S*)-**1** would selectively oxidize at an alternative site, providing a distinct functional group handle for further chemical modification. High levels of regio-, chemo-, and stereoselectivity were observed in the oxidation of pleuromutilin derivative dihydropleuromutilone [(−)-**56**)] with (*S,S*)-**1**/$H_2O_2$ (Fig. 4, D and E). The C14 glycolic acid side chain, a prevalent site for chemical modification, remained intact during oxidation. This result illustrates the extraordinary chemoselectivity possible with this oxidant; even a primary alcohol can be electronically deactivated from oxidation when α to a carbonyl. Electron-withdrawing carbonyl and ester moieties effectively deactivate the five- and eight-membered rings toward electrophilic oxidation with (*S,S*)-**1**/$H_2O_2$, rendering the six-membered ring as the mostly likely region for oxidation. Although the axial tertiary C–H bond at C6 is electronically accessible, it is situated in the sterically congested cavity of the five- and six-membered fused ring system (Fig. 4D). We hypothesized that the C7 methylene is the single most electron-rich and sterically accessible site for oxidation by catalyst (*S,S*)-**1**/$H_2O_2$. Consistent with this analysis, we observed that 62% of the starting material is oxidized specifically at C7 (24% rsm) among 11 possible sites of oxidation. The major oxidation product is the result of diastereoselective hydroxylation at the more sterically accessible equatorial secondary C–H bond, providing (−)-**57** as a single isomer in 42% isolated yield (Fig. 4E). In comparison, ketone at C7 [(−)-**58**] is provided in only 20% yield. Although the C–H bond of a secondary alcohol is highly electronically activated toward oxidation, energy minimization of (−)-**56** shows that this bond is sterically deactivated by virtue of its proximity to the eight-membered ring (Fig. 4D).

A small-molecule reagent sensitive to the local chemical environment of the substrate has enabled selective methylene C–H oxidations that are predictable using the fundamental concepts of electronics, sterics, and stereoelectronics. We anticipate that these findings will contribute to redefining how C–H bonds are viewed in synthetic planning, future methods development, and the exploration of molecular diversity.

### References and Notes

1. J. Clardy, C. Walsh, *Nature* **432**, 829 (2004).
2. P. R. Ortiz de Montellano, Ed., *Cytochrome P450: Structure, Mechanism and Biochemistry* (Plenum, New York, ed. 3, 2005).
3. M. S. Chen, M. C. White, *Science* **318**, 783 (2007).

4. N. A. Vermeulen, M. S. Chen, M. C. White, *Tetrahedron* **65**, 3078 (2009).
5. R. Mello, M. Fiorentino, C. Fusco, R. Curci, *J. Am. Chem. Soc.* **111**, 6749 (1989).
6. D. H. R. Barton, E. Csuhai, N. Ozbalik, *Tetrahedron* **46**, 3743 (1990).
7. C. Kim, K. J. Chen, J. Kim, L. Que Jr., *J. Am. Chem. Soc.* **119**, 5964 (1997).
8. T. Okuno, S. Ito, S. Ohba, Y. Nishida, *J. Chem. Soc. Dalton Trans.* **1997**, 3547 (1997).
9. Exo selective oxidations of norbornyl derivatives have been observed under Fenton conditions (iron salts with $H_2O_2$) (*32*).
10. J. P. Collman, H. Tanaka, R. T. Hembre, J. I. Brauman, *J. Am. Chem. Soc.* **112**, 3689 (1990).
11. A rare example of regioselective, unactivated methylene oxidation has been reported. Using an iron porphyrin catalyst, hexane oxidation using excess substrate gave 2-hexanol and 3-hexanol in 13 and 7% yields, respectively, based on oxidant (*33*).
12. M. S. Chen, M. C. White, *J. Am. Chem. Soc.* **126**, 1346 (2004).
13. K. J. Fraunhoffer, D. A. Bachovchin, M. C. White, *Org. Lett.* **7**, 223 (2005).
14. E. M. Stang, M. C. White, *Nat. Chem.* **1**, 547 (2009).
15. M. A. Umbreit, K. B. Sharpless, *J. Am. Chem. Soc.* **99**, 5526 (1977).
16. S. Das, C. D. Incarvito, R. H. Crabtree, G. W. Brudvig, *Science* **312**, 1941 (2006).
17. J. Yang, B. Gabriele, S. Belvedere, Y. Huang, R. Breslow, *J. Org. Chem.* **67**, 5057 (2002).
18. L. V. Desai, K. L. Hull, M. S. Sanford, *J. Am. Chem. Soc.* **126**, 9542 (2004).
19. K. Chen, P. S. Baran, *Nature* **459**, 824 (2009).
20. B. H. Brodsky, J. Du Bois, *J. Am. Chem. Soc.* **127**, 15391 (2005).
21. R. Mas-Ballesté, L. Que Jr., *Science* **312**, 1885 (2006).
22. For the beneficial effects of AcOH on nonheme iron-catalyzed oxidations (olefin epoxidation), see (*34*).
23. Materials and methods are available as supporting material at *Science* Online.
24. E. L. Eliel, S. H. Schroeter, T. J. Brett, F. J. Biros, J. C. Richer, *J. Am. Chem. Soc.* **88**, 3327 (1966).
25. G. A. Olah, P. Reddy, G. K. S. Prakash, *Chem. Rev.* **92**, 69 (1992).
26. P. A. Wender, M. K. Hilinski, A. V. W. Mayweg, *Org. Lett.* **7**, 79 (2005).
27. J. S. Lee, P. L. Fuchs, *Org. Lett.* **5**, 2247 (2003).
28. E. M. Davis, R. Croteau, *Top. Curr. Chem.* **209**, 53 (2000).
29. A. Farooq, S. Tahara, *Z. Naturforsch. C* **55**, 341 (2000).
30. A. Ata, L. J. Conci, J. Betteridge, I. Orhan, B. Sener, *Chem. Pharm. Bull. (Tokyo)* **55**, 118 (2007).
31. R. L. Hanson *et al.*, *Org. Process Res. Dev.* **6**, 482 (2002).
32. J. T. Groves, T. E. Nemo, R. S. Myers, *J. Am. Chem. Soc.* **101**, 5290 (1979).
33. M. H. Lim, Y. J. Lee, Y. M. Goh, W. Nam, C. Kim, *Bull. Chem. Soc. Jpn.* **72**, 707 (1999).
34. M. C. White, A. G. Doyle, E. N. Jacobsen, *J. Am. Chem. Soc.* **123**, 7194 (2001).
35. Dedicated to Professor Eric N. Jacobsen on his 50th birthday for his inspirational work on selective oxidations. We gratefully acknowledge R. J. Pakula for performing gas chromatography experiments toward elucidating the steric effects on oxidation site selectivity; M. A. Bigi, D. J. Covell, and E. M. Stang for helpful discussions and checking our spectroscopic data; and S. A. Reed for helpful discussions and checking our experimental procedure. M.S.C. was a Harvard University graduate student who completed his doctoral work with M.C.W. at the University of Illinois at Urbana-Champaign. This work was submitted to M.S.C.'s committee as part of his thesis on 28 August 2009 and was presented by M.C.W. at the Welch Symposium on 27 October 2009. We are grateful to the A. P. Sloan Foundation, the Camille and Henry Dreyfus Foundation, Bristol-Myers Squibb, Pfizer, Abbott, and the University of Illinois for financial support. M.S.C. is a 2008 Bristol-Myers Squibb Graduate Fellow in Synthetic Organic Chemistry. A U.S. patent on "Selective Aliphatic C–H Oxidation" is pending (application 12/245,086).

**Supporting Online Material**

www.sciencemag.org/cgi/content/full/327/5965/566/DC1
Materials and Methods
References

20 October 2009; accepted 25 November 2009
10.1126/science.1183602

# A Basal Alvarezsauroid Theropod from the Early Late Jurassic of Xinjiang, China

**Jonah N. Choiniere,[1]* Xing Xu,[2] James M. Clark,[1] Catherine A. Forster,[1] Yu Guo,[2] Fenglu Han[2]**

**The fossil record of Jurassic theropod dinosaurs closely related to birds remains poor. A new theropod from the earliest Late Jurassic of western China represents the earliest diverging member of the enigmatic theropod group Alvarezsauroidea and confirms that this group is a basal member of Maniraptora, the clade containing birds and their closest theropod relatives. It extends the fossil record of Alvarezsauroidea by 63 million years and provides evidence for maniraptorans earlier in the fossil record than *Archaeopteryx*. The new taxon confirms extreme morphological convergence between birds and derived alvarezsauroids and illuminates incipient stages of the highly modified alvarezsaurid forelimb.**

The presence of the basal avialan (*1*–*3*) *Archaeopteryx* in the latest Late Jurassic (Tithonian) and the poor fossil representation of more basal maniraptoran taxa in contemporaneous or slightly older deposits indicate either a gap in the stratigraphic record or, more controversially, that birds are not related to theropods (*4*). Recent discoveries of Middle-Late Jurassic maniraptorans (*5*–*7*) from China are starting to fill in the temporal gap, but the ages of these new taxa are poorly resolved (*8*, *9*), and they do not clarify basal maniraptoran diversification because very little character evidence separates them from birds (*5*, *7*).

[1]Department of Biological Sciences, The George Washington University, Washington, DC 20052, USA. [2]Key Laboratory of Evolutionary Systematics of Vertebrates, Institute of Vertebrate Paleontology and Paleoanthropology, Beijing 100044, China.

*To whom correspondence should be addressed. E-mail: jonah.choiniere@gmail.com

Here, we describe a three-dimensionally preserved, nearly complete skeleton of an alvarezsauroid theropod, *Haplocheirus sollers*, gen. et spec. nov. (*10*), from orange mudstone beds in the upper part of the Shishugou Formation in Wucaiwan area, Junggar Basin, Xinjiang, China. Radiometric dating constrains the age of this fossil to between 158.7 ± 0.3 and 161.2 ± 0.2 Ma (million years ago) (*11*), corresponding to the Oxfordian marine stage in the early Late Jurassic (*12*). The dates for *Haplocheirus* reduce the conflict between the fossil record and phylogenetic hypotheses that early maniraptoran diversification took place in the Jurassic. Alvarezsauroids are known from South America (*13*–*15*), Asia (*16*–*19*), North America (*20*, *21*), and Europe (*22*, *23*). The basal phylogenetic position and early temporal position of *Haplocheirus* imply that Alvarezsauroidea originated in Asia rather than South America (*14*, *20*). Derived members of the Alvarezsauroidea were originally thought to be flightless basal avialans (*18*) because they share many morphological characteristics with birds, including a loosely sutured skull, a keeled sternum, fused wrist elements, and a posteriorly directed pubis. *Haplocheirus* preserves plesiomorphic morphological characteristics that confirm a basal position for Alvarezsauroidea within Maniraptora (*24*), demonstrating that these features of derived alvarezsauroids represent dramatic convergences with birds.

IVPP (Institute of Vertebrate Paleontology and Paleoanthropology) V15988 (Figs. 1 and 2 and figs. S4 to S9) is ~140 cm in total body length as preserved but is missing the end of the tail (estimated total length 190 to 230 cm; table S1). The bones of the braincase are coossified and the neurocentral sutures are visible, suggesting that the animal is likely a young adult or late-stage subadult.

The gracile, low skull (Fig. 2A and figs. S4 to S7) is well preserved in three dimensions. The narrow, elongate rostrum becomes taller and wider just anterior to the large, anterolaterally facing orbits. The dorsoventrally thin jugal is triradiate, unlike the rodlike jugal of more derived alvarezsauroids (*17*). In lateral view, the basisphenoid is oriented at 45° to horizontal, a condition present in some troodontids (*25*) and in alvarezsauroids (*17*). The basipterygoid processes are long and project ventrolaterally, a morphology known only in primitive birds and alvarezsauroids among Theropoda (*17*).

At least 30 small maxillary teeth are present in *Haplocheirus*, as in *Shuvuuia* (*17*), *Pelecanimimus* (*26*), therizinosauroids (*27*), and troodontids (*28*). Unlike the conical, unserrated teeth of *Mononykus* (*28*) and *Shuvuuia* (*29*), however, the maxillary teeth of *Haplocheirus* are